Amplifying ultraweak transitions in collective systems via quantum interference

Ni Cui[1,2,3,*] and Mihai A. Macovei[1,4,†]

[1]*Max-Planck-Institut für Kernphysik, Saupfercheckweg 1, 69117 Heidelberg, Germany*

[2]*Siyuan Laboratory, Guangzhou Key Laboratory of Vacuum Coating Technologies and New Energy Materials, Department of Physics, Jinan University, Guangzhou 510632, China*

[3]*Guangdong Provincial Key Laboratory of Optical Fiber Sensing and Communications, Jinan University, Guangzhou 510632, China*

[4]*Institute of Applied Physics, Academy of Sciences of Moldova, Academiei Street 5, 2028 Chişinău, Moldova*

(Received 6 March 2017; published 11 December 2017)

We investigate laser-induced quantum interference phenomena in superradiance processes evolving in an ensemble of initially excited Λ-type closely packed three-level emitters. The lower doublet levels are pumped with a coherent laser field. Due to constructive quantum interference effects, the superradiance occurs in a much weaker atomic transition, which is not the case in the absence of the coherent driving. This result may be of visible relevance for enhancing ultraweak transitions in atomic or atomiclike systems or for high-frequency lasing effects.

DOI: 10.1103/PhysRevA.96.063814

I. INTRODUCTION

Vacuum-induced correlations among closely spaced quantum emitters forming an ensemble lead to significant changes in the quantum dynamics [1–7]. In this context, the superradiance, an already well-known phenomenon, emphasizes the fast decay of an initially excited cooperative system as well as an enhanced radiation intensity. An enormous number of experimental and theoretical works were performed with respect to this issue and superradiance behaviors were found in a wide range of different systems and for various applications [8–17]. The collective quantum dynamics can be manipulated by applying external coherent laser sources. In particular, triggering of the superradiance phenomenon nicely occurs in a three-level V-type atomic ensemble when an external coherent field pumps one of the atomic transitions [18]. In a somehow related setup, superfluorescence without inversion was shown to occur as well [19] (see also [20]). One may anticipate cooperative effects in novel systems because x-ray free-electron lasers may accelerate the decay of a nuclear isomer [21]. Furthermore, in a large ensemble of nuclei operating in the x-ray regime and resonantly coupled to a common cavity environment, two fundamentally different mechanisms related to cooperative emission and magnetically controlled anisotropy of the cavity vacuum have been responsible for fascinating effects mainly related to quantum interference phenomena [22]. Actually, these effects originate from the indistinguishability of the corresponding transition pathways [5,6,22,23].

Interfering transition amplitudes can be used in principle to detect weak atomic interactions like measurements of magnetic dipole interactions, quadrupole interactions, or weak atomic transitions occurring, for instance, because of parity-violation effects as well as to identify various nonlinear transition channels [24–27]. Furthermore, ultranarrow absorption lines due to an electromagnetically induced transparency phenomenon were shown to be very useful for high-accuracy optical clocks [28]. Recently, superradiance on the millihertz linewidth strontium clock transition was shown to occur in [29]. This was achieved with the help of an optical cavity which triggered the superradiance on the ultraweak transition. Somehow related, prospects for millihertz-linewidth lasers were suggested too in [30].

Under these circumstances, we discuss here a setup where weak or ultraweak decaying transitions can be significantly enhanced in an initially excited ensemble of few-level collectively interacting Λ-type atoms. Notably, the effect arises due to quantum interference phenomena among different decaying pathways which are induced by the coherent pumping of the two lower levels. The rapid time evolution of an ultraslow atomic transition is determined by the fast decay rate of another transition of the Λ sample. Moreover, the effect is of a cooperative nature and it is absent in excited single-atom systems or independent atomic ensembles. In particular, we have found that (i) the superradiance of the ultraweak transition may take place when there are more atoms in the ground state than in the excited one, (ii) the superradiance peak occurs when the population of the excited level is trapped and almost constant during a short time which is distinct from the standard superradiance phenomenon where its time-dependent intensity relies on the fast population slope, and (iii) quantum coherences induced by the coherent pumping are responsible for superradiant population transfer of the ultraweak transition as well as among the lower sublevels during the superradiant burst. As possible applications of our results we suggest enhancing dipole-forbidden or any other ultraweak transitions, quantum clock atomic systems, and high-frequency lasing. In the case of dipole-forbidden transitions, correlated photons can be generated at an enhanced rate.

This paper is organized as follows. In Sec. II, we describe the analytic model and analyze the relevant equations of motion using the system's master equation. In Sec. III, we numerically solve those equations and discuss the resulting collective dynamics and feasible applications. A summary is given in Sec. IV.

II. ANALYTICAL FRAMEWORK

We consider an initially excited ensemble of N identical Λ-type three-level emitters, each consisting of states $|1\rangle$, $|2\rangle$,

*cuinicn@gmail.com

†macovei@phys.asm.md

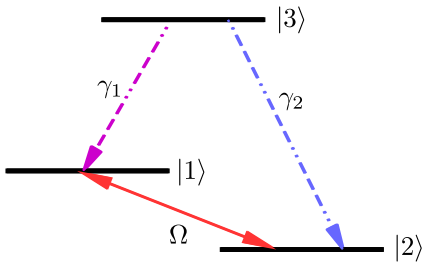

FIG. 1. Energy levels of the Λ-type three-level system. Here γ_1 and γ_2, $\gamma_1 \gg \gamma_2$, are the single-atom spontaneous decay rates of transitions $|3\rangle \to |1\rangle$ and $|3\rangle \to |2\rangle$, respectively. The coherent laser field drives the $|1\rangle \leftrightarrow |2\rangle$ transition, with Ω the corresponding Rabi frequency.

and $|3\rangle$, as depicted in Fig. 1. The lower doublet transition $|2\rangle \leftrightarrow |1\rangle$ is resonantly driven by a cw coherent laser field or a long pulse with time duration $\tau > \gamma_1^{-1}$. The emitters can decay via a fast dipole-allowed $|3\rangle \leftrightarrow |1\rangle$ transition as well as through a slow or ultraslow $|3\rangle \leftrightarrow |2\rangle$ atomic transition due to coupling with the environmental vacuum modes. The interparticle separations are of the order of or smaller than the relevant emission wavelengths of the system, and in this way the atomic sample acquires a cooperative nature.

In the usual mean-field, Born-Markov, and rotating-wave approximations, our model is described by the master equation [2–6]

$$\dot{\rho}(t) + i\Omega \sum_{j=1}^{N} \left[S_{12}^{(j)} + S_{21}^{(j)}, \rho\right] = -\sum_{j,l=1}^{N} \left\{\gamma_{jl}^{(1)}\left[S_{31}^{(j)}, S_{13}^{(l)}\rho\right] + \gamma_{jl}^{(2)}\left[S_{32}^{(j)}, S_{23}^{(l)}\rho\right]\right\} + \text{H.c.} \quad (1)$$

Here Ω is the corresponding Rabi frequency, while $\gamma_{jl}^{(s)} \equiv \gamma_s[\aleph_{jl}^{(s)} + i\Omega_{jl}^{(s)}]$ ($s \in \{1,2\}$) are the collective parameters with $\aleph_{jl}^{(s)}$ and $\Omega_{jl}^{(s)}$ describing the mutual interactions among emitter pairs $\{j,l\}$. For dipole-allowed transitions, for instance, one has $\aleph_{jl}^{(s)} = \sin(\omega_{3s} r_{jl}/c)/(\omega_{3s} r_{jl}/c)$ and $\Omega_{jl}^{(s)} = -\cos(\omega_{3s} r_{jl}/c)/(\omega_{3s} r_{jl}/c)$, where we have averaged over all dipole orientations and $r_{jl} = |\vec{r}_j - \vec{r}_l|$ are the interparticle intervals between the jth and the lth emitters, respectively [2–9]. For a dipole-forbidden transition one may refer to [31–33]. Further, $\omega_{\alpha\beta}$, with $\{\alpha,\beta\} \in \{1,2,3\}$, is the frequency of the $|\beta\rangle \leftrightarrow |\alpha\rangle$ atomic transition. Here $S_{\alpha\beta}^{(j)} = |\alpha\rangle_{jj}\langle\beta|$ represents the population of the state $|\alpha\rangle$ in the jth atom, if $\alpha = \beta$, or the transition operator from $|\beta\rangle$ to $|\alpha\rangle$ of the jth atom when $\alpha \neq \beta$. The atomic operators obey the commutation relations $[S_{\alpha\beta}^{(j)}, S_{\beta'\alpha'}^{(l)}] = \delta_{jl}(\delta_{\beta\beta'} S_{\alpha\alpha'}^{(j)} - \delta_{\alpha\alpha'} S_{\beta'\beta}^{(j)})$. Correspondingly, γ_1 and γ_2 are the single-atom spontaneous decay rates of the $|3\rangle \to |1\rangle$ and $|3\rangle \to |2\rangle$ atomic transitions.

In the following, we will use Eq. (1) to investigate the collective dynamics of an initially excited ensemble of Λ-type emitters when $\gamma_1 \gg \gamma_2$.

A. Single-atom case

For the sake of comparison, we first consider a single-atom case. The spontaneous decay law of an initially excited atom is given by the expression

$$\langle S_{33}(t)\rangle = \langle S_{33}(0)\rangle \exp[-2(\gamma_1 + \gamma_2)t], \quad (2)$$

where $\langle S_{33}(0)\rangle$ denotes the initial population on the $|3\rangle$ level. This means that in the case of a fully excited atom there is no way to influence the decay law of the upper state via applying a coherent laser field on the lower doublet levels. Furthermore, for a purely spontaneous decaying system the ratio of the lower-state populations is $\langle S_{11}(t)\rangle/\langle S_{22}(t)\rangle = \gamma_1/\gamma_2$, i.e., these states will be spontaneously populated depending on the corresponding decay rates [34]. The spontaneous electromagnetic field intensities on these transitions are proportional to the population of the lower states during the spontaneous decay. Applying a coherent laser field on the lower doublet states, with the atom being initially in the upper excited state $|3\rangle$, the population among the lower energy levels will oscillate after a while in the usual way.

B. Multiatom case

In what follows, we will see how these processes modify in the case of a collectively interacting atomic ensemble. We will continue by considering an ensemble of emitters with a higher density, i.e., $n \sim \lambda_2^{-3}$, such that the emitters of both involved transitions $|3\rangle \to |1\rangle$ and $|3\rangle \to |2\rangle$ interact collectively. Here λ_2 (or λ_1) is the corresponding wavelength on transition $|3\rangle \to |2\rangle$ ($|3\rangle \to |1\rangle$). Initially, the emitters are prepared in the excited state $|3\rangle$ and $\gamma_1 \gg \gamma_2$. The dynamics of the cooperative decay of both transitions $|3\rangle \to |1\rangle$ and $|3\rangle \to |2\rangle$ is obtained with the help of the master equation (1) via decoupling of higher-order atomic correlators, an approach valid for $N \gg 1$ [4]. In particular, the equations for the populations and coherences $\langle S_{\alpha\alpha'}\rangle/N = \sum_{j=1}^{N}\langle S_{\alpha\alpha'}^{(j)}\rangle/N$, $\{\alpha,\alpha' \in 1,2,3\}$, and the intensity of the superradiant emission $I_\beta \propto \langle S_{3\beta} S_{\beta 3}\rangle/N^2 = \sum_{j,l=1(j\neq l)}^{N}\langle S_{3\beta}^{(j)} S_{\beta 3}^{(l)}\rangle/N^2$, $\beta \in \{1,2\}$, are governed by the number of collectively interacting emitters N, some geometrical factors $\{\mu_1,\mu_2\}$ [3,4], the decay rates $\{\gamma_1,\gamma_2\}$, and the Rabi frequency Ω. To give some clarification regarding the system of equations used to describe our sample, we present a few terms in the equations of motion describing the population in the state $|1\rangle$ and the intensity of the $|3\rangle \to |1\rangle$ transition, namely, $(d/dt)\langle S_{11}\rangle = \cdots \sum_{l,k\,(l\neq k)}^{N} \gamma_{kl}^{(1)}\langle S_{31}^{(l)} S_{13}^{(k)}\rangle + \text{H.c.}$, $(d/dt)\langle S_{31} S_{13}\rangle = \cdots - \sum_{l,m,n\,(l\neq m\neq n)}^{N} \gamma_{ml}^{(1)}\langle S_{31}^{(l)} S_{13}^{(n)}(S_{11}^{(m)} - S_{33}^{(m)})\rangle - \sum_{l,m,n\,(l\neq m\neq n)}^{N} \gamma_{ml}^{(2)}\langle S_{32}^{(l)} S_{13}^{(n)} S_{21}^{(m)}\rangle + \text{H.c.}$, and so on. Here $\langle S_{11}\rangle = \sum_{j=1}^{N}\langle S_{11}^{(j)}\rangle$, whereas $\langle S_{31} S_{13}\rangle = \sum_{j\neq l}^{N}\langle S_{31}^{(j)} S_{13}^{(l)}\rangle$. Correspondingly, the equations of motion for the population dynamics in the state $|2\rangle$ and the intensity of the $|3\rangle \to |2\rangle$ transition can be obtained via exchanging the indices $1 \leftrightarrow 2$. One can observe that the equation of motion for a certain-order atomic correlator is represented through higher-order ones. To obtain a closed system of equations we decoupled the three-particle correlators as follows: $\langle S_{31}^{(l)} S_{13}^{(n)}(S_{11}^{(m)} - S_{33}^{(m)})\rangle \approx \langle S_{31}^{(l)} S_{13}^{(n)}\rangle\langle(S_{11}^{(m)} - S_{33}^{(m)})\rangle$ and $\langle S_{32}^{(l)} S_{13}^{(n)} S_{21}^{(m)}\rangle \approx \langle S_{32}^{(l)} S_{13}^{(n)}\rangle\langle S_{21}^{(m)}\rangle$. The strategy of the decoupling procedure consists in trying to get a minimal system of equations of motion for a particular decoupling scheme, i.e., in our case the decoupling is applied to

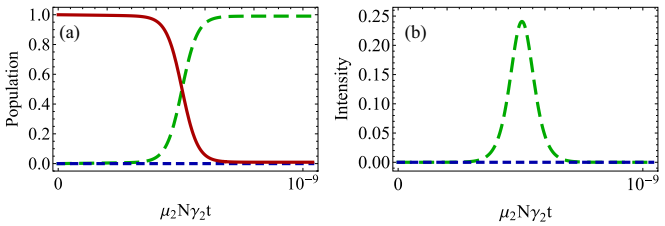

FIG. 2. (a) Collective population on the state $|1\rangle$ (green long-dashed curve), the state $|2\rangle$ (blue short-dashed line), and the state $|3\rangle$ (red solid curve) and (b) the superradiant intensities on transitions $|3\rangle \to |1\rangle$ (green long-dashed curve) and $|3\rangle \to |2\rangle$ (blue short-dashed line) as a function of the scaled time $\mu_2 N\gamma_2 t$. Here $\Omega = 0$, $\gamma_2/\gamma_1 = 10^{-8}$, $\mu_2/\mu_1 = 1/16$, $\mu_2 = 10^{-5}$, and $\langle S_{33}(0)\rangle = N = 10^7$.

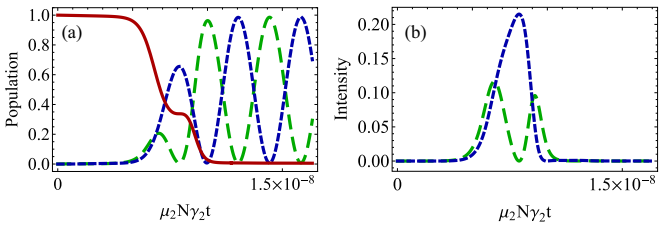

FIG. 3. Same as in Fig. 2 but for $\Omega/\mu_1\gamma_1 N = 0.47$.

three-particle correlators (one can, for instance, start decoupling the four-particle correlators, etc.). At the end, we will arrive at a nonlinear system of 12 equations of motion, which are solved numerically. This method is widely used to characterize multiparticle ensembles [4] and adequately describes collective intensities, populations, fast decay, etc., in the Dicke model or related systems or modifications.

III. RESULTS AND FEASIBLE APPLICATIONS

In the absence of the coherent driving, i.e., $\Omega = 0$, the time evolution of populations of the states $|1\rangle$, $|2\rangle$, and $|3\rangle$ and the collective intensities of the transitions $|3\rangle \to |1\rangle$ and $|3\rangle \to |2\rangle$ are presented in Figs. 2(a) and 2(b), respectively, when $\gamma_1 \gg \gamma_2$. One can observe typical superradiant behaviors, that is, the population in the state $|3\rangle$ will cooperatively decay to the state $|1\rangle$, rapidly followed concomitantly by a superradiant pulse emission in the transition $|3\rangle \to |1\rangle$ [see, respectively, the solid red curve in Fig. 2(a) and the green long-dashed lines in Figs. 2(a) and Fig. 2(b)]. However, there is no superradiant emission in the transition $|3\rangle \to |2\rangle$ [see the blue short-dashed lines in Figs. 2(a) and 2(b)]. These behaviors can be well understood in the Dicke limit [4]. For an initially excited large atomic ensemble, i.e., $\langle S_{33}(0)\rangle = N$ and $N \gg 1$, one has

$$\langle S_{\alpha\alpha}(t)\rangle + 1 = [\langle S_{\beta\beta}(t)\rangle + 1]^{\gamma_\alpha/\gamma_\beta}, \tag{3}$$

with $\alpha \neq \beta \in \{1,2\}$. It is easily to observe that if $\gamma_1 = \gamma_2$ we always have $\langle S_{11}(t)\rangle = \langle S_{22}(t)\rangle$. For longer time durations and when $\gamma_1 \ll \gamma_2$ one has that $\langle S_{11}(t)\rangle \to 0$ whereas $\langle S_{22}(t)\rangle \to N$, and vice versa, i.e., for $\gamma_1 \gg \gamma_2$, $\langle S_{22}(t)\rangle \to 0$ while $\langle S_{11}(t)\rangle \to N$.

Now we add a cw coherent laser field to couple the lower levels $|1\rangle \leftrightarrow |2\rangle$. If the Rabi frequency Ω is considerably smaller than the collective decay rates, i.e., $\Omega \ll \mu_1\gamma_1 N$, there is only a very small number of emitters decaying to the ground state $|2\rangle$ with a weak superradiant burst in the transition $|3\rangle \to |2\rangle$, somehow similar to the picture described above. However, when the Rabi frequency is comparable to but still smaller than the collective decay rate, i.e., $\Omega < \mu_1\gamma_1 N$, the population dynamics is quite different from the case of smaller Rabi frequencies. In particular, Figs. 3(a) and 3(b) depict the evolution of collective populations in the states $|1\rangle$, $|2\rangle$, and $|3\rangle$, as well as the intensities of the superradiant emissions for a particular value of the Rabi frequency, that is, for $\Omega/\mu_1\gamma_1 N = 0.47$. Compared with the case $\Omega = 0$ in Fig. 2(a), the population in the excited state $|3\rangle$ decreases to zero over a longer time and with a small visible plateau [see the red solid curve in Fig. 3(a)]. In contrast, the population in the state $|2\rangle$ [blue short-dashed line in Fig. 3(a)] increases. The superradiance features behave accordingly. Remarkably, there is a strong superradiant pulse occurring in the much weaker transition $|3\rangle \to |2\rangle$ [see the blue short-dashed curve in Fig. 3(b)]. Notice that the superradiant behaviors shown in Fig. 3 differ from the ordinary superradiance in the sense that it is not quite determined by the fast population slope of the excited level since, in our case, the excited-state population has almost a constant value when the superradiance peak occurs [without a coherent applied field, the superradiant intensity I is proportional to $I \propto -\partial\langle S_z(t)\rangle/\partial t$ for two-level emitters, where $\langle S_z(t)\rangle$ is the collective inversion operator]. Although the uppermost-state population has a small plateau during a short time interval [see the red solid curve in Fig. 3(a)], the population from the state $|1\rangle$ transfers to $|2\rangle$ [see the long- and short-dashed curves in Fig. 3(a)], while the superradiance pulse achieves its maximum in the $|3\rangle \leftrightarrow |2\rangle$ transition [see the blue short-dashed line in Fig. 3(b)]. More specifically, if one inspects the populations in states $|1\rangle$ and $|2\rangle$, that is, $\langle S_{11}\rangle$ and $\langle S_{22}\rangle$ depicted in Fig. 3(a), then these populations increase until they reach a maximum in the state $|1\rangle$, that is, when $\langle S_{11}\rangle/N = \langle S_{22}\rangle/N \approx 0.2$. In the subsequent moment, the population from the state $|1\rangle$ is then completely transferred to $|2\rangle$, which means that in the state $|2\rangle$ we should have approximately $\langle S_{22}\rangle/N \approx 0.2 + 0.2 = 0.4$. Careful inspection of Fig. 3(a), in the time moment where the population in the state $|1\rangle$ is zero, shows that the population in the state $|2\rangle$ is $\langle S_{22}\rangle/N > 0.6$. Thus, one can conjecture that the level $|2\rangle$ populates via two interfering decay channels: a direct one $|3\rangle \to |2\rangle$ and an indirect one $|3\rangle \to |1\rangle \to |2\rangle$. Furthermore, there are more atoms in the ground state $|2\rangle$ than in the excited one when the superradiant maximum takes place in the ultraslow transition (see Fig. 3). Again, this is distinct from standard superradiance features found in a two-level sample where the population is distributed equally when the superradiance peak occurs. Further, the intensity of the fast decaying transition vanishes in addition to the population in the level $|1\rangle$ during the superradiant burst in the ultraslow transition (see Fig. 3). Additionally, due to the strong coupling between the states $|1\rangle$ and $|2\rangle$, the superradiant pulse in the fast transition $|3\rangle \to |1\rangle$ splits into two pulses [see the green long-dashed curve in Fig. 3(b)]. At the final stage, when the population in the state $|3\rangle$ reduces to zero, Rabi oscillations occur naturally between the states $|1\rangle$ and $|2\rangle$. These behaviors do not change much as long as $\Omega/\mu_1\gamma_1 N \sim 1/2$.

The results described above can be physically explained in the semiclassical dressed-state picture. The corresponding eigenvectors due to laser dressing of atoms on lower doublet levels can be written in terms of the bare states, namely, $|\pm\rangle = \frac{1}{\sqrt{2}}(|2\rangle \pm |1\rangle)$. The energy difference between the two dressed states depends on the Rabi frequency of the driving coherent laser field Ω. The population in the excited state $|3\rangle$ would decay to the two dressed states $|\pm\rangle$, which are a mixture of the bare states $|1\rangle$ and $|2\rangle$. Therefore, in the dressed-state picture, the intensity of the superradiant pulses in the transitions $|3\rangle \to |1\rangle$ and $|3\rangle \to |2\rangle$ can be expressed as

$$I_{1\,(2)} \propto \langle R_{3-}R_{-3}\rangle + \langle R_{3+}R_{+3}\rangle \mp \langle R_{3-}R_{+3}\rangle \mp \langle R_{3+}R_{-3}\rangle. \tag{4}$$

Here $R_{3\pm} = \sum_{j=1}^{N} |3\rangle_{jj}\langle\pm|$ $(R_{\pm 3} = \sum_{j=1}^{N} |\pm\rangle_{jj}\langle 3|)$ are the collective transition operators from the dressed states $|\pm\rangle \to |3\rangle$ $(|3\rangle \to |\pm\rangle)$ of each emitter j. It follows from expression (4) that the intensities of the superradiant pulses, while atoms decay from state $|3\rangle$ to states $|1\rangle$ and $|2\rangle$, include two parts: One part is the superradiance from state $|3\rangle$ to the dressed states $|\pm\rangle$ and the other part describes the contribution to the superradiant emission due to quantum coherences between the two decaying paths which are induced by the driving coherent source. When the Rabi frequency Ω is large, the emitters in the excited state $|3\rangle$ would decay via independent channels to the dressed states $|\pm\rangle$ because the cross correlations between the two channels average to zero. In this case, two superradiant pulses with carrier frequencies $\omega_{3\alpha} \pm 2\Omega$ are generated on each bare state transition, however, their magnitudes are different because of the prefactor proportional to γ_α, $\alpha \in \{1,2\}$. For smaller Rabi frequency $\Omega < \mu_1\gamma_1 N$, the two possible decaying pathways became indistinguishable such that the decay amplitudes from the excited state $|3\rangle \to |\pm\rangle$ interfere with each other. These collective decay-induced coherences may give rise to quantum interference between the two decaying paths. Actually, those decay-induced coherences lead to constructive quantum interference in the transition $|3\rangle \to |2\rangle$ and to destructive quantum interference in the transition $|3\rangle \to |1\rangle$. That is why, for smaller Rabi frequencies, i.e., $\Omega = 0.47\mu_1\gamma_1 N$, a strong superradiant emission occurs in the much weaker transition $|3\rangle \to |2\rangle$, while the superradiant pulse in the transition $|3\rangle \to |1\rangle$ splits into two pulses. The induced quantum coherences are responsible for population transfer among the lower doublet levels when the superradiant burst takes place, while the higher upper-state population is almost constant. The whole cooperative process lasts over a time period determined by the inverse of the faster collective decay rate. Notice that the cross correlations between the two involved decay channels in expression (4) vanish for a single-atom system (or many independent emitters), i.e., $R_{3-}R_{+3} = |3\rangle\langle -||+\rangle\langle 3| = 0$ and $R_{3+}R_{-3} = (R_{3-}R_{+3})^{\dagger}$, when $N = 1$. Therefore, the effect described here is purely of the collective nature. Now we would like to compare the intensities emitted in the ultraweak transition for independent emitters $I_{2\,\mathrm{ind}}$ or collectively interacting ones $I_{2\,\mathrm{col}}$. In the first case the intensity is $I_{2\,\mathrm{ind}} = \hbar\omega_{32}\gamma_2 N\langle S_{22}\rangle$, where $\langle S_{22}\rangle$ is the mean value of the single-atom population in the state $|2\rangle$. Taking into account that for independent or single-atom systems $\langle S_{22}\rangle/\langle S_{11}\rangle = \gamma_2/\gamma_1$, one has that $\langle S_{22}\rangle = (\gamma_2/\gamma_1)/(1+\gamma_2/\gamma_1)$. Thus, in this case, $I_{2\,\mathrm{ind}} = \hbar\omega_{32}\gamma_2 N(\gamma_2/\gamma_1)/(1+\gamma_2/\gamma_1)$. For $\gamma_2/\gamma_1 = 10^{-8}$ and $N = 10^7$, we have that $I_{2\,\mathrm{ind}} = 0.1\hbar\omega_{32}\gamma_2$. For a collectively interacting ensemble, the peak intensity of the ultraweak transition $|3\rangle \to |2\rangle$ can be estimated as $I_{2\,\mathrm{col}} = \hbar\omega_{32}\gamma_2\mu_2 N^2$. For the same parameters as in Fig. 3(b), one has that $I_{2\,\mathrm{col}} = 0.2\hbar\omega_{32}\gamma_2 \times \mu_2 N \times N = 0.2\hbar\omega_{32}\gamma_2 \times 100 \times N = 20\hbar\omega_{32}\gamma_2 N$, which is significantly bigger than that for an independent atomic ensemble.

To create population inversions up to moderate x rays, frequencies may not be principally too hard because of available coherent light sources. Therefore, in these frequency ranges, our scheme may be applied for cooperative lasing or towards amplifying ultraslow atomic transitions like dipole-forbidden ones or due to parity-violating effects [24–26]. In particular, in the case of dipole-forbidden transitions, quantum correlated photons can be generated at an increased rate and intensity (see [32,33]). Enhancing ultraweak transitions in quantum clock systems may be another option [28,29]. One may use a Λ-type system containing ultranarrow optical transitions in alkaline-earth atoms (Sr, Yb, Ca, etc.), for instance [35]. For higher-frequency effects it turns out that obtaining population inversion is quite challenging, although one may proceed in the same vein as suggested in [36] to excite high-lying energy levels in γ diapason. To this end, note a recently proposed promising scheme to achieve nuclei population inversion at keV frequencies [37].

IV. SUMMARY

We have investigated the superradiance effect occurring in a closely spaced Λ-type atomic ensemble. The single-atom spontaneous decay rates to the lower doublet states are different. For an initially excited system, the superradiance phenomenon takes place mainly in the transition possessing a higher spontaneous decay rate. We have found that when a coherent laser field is applied to the lower doublet states, the superradiance is surprisingly enhanced in the much weaker atomic transition. This effect is identified with quantum interference effects among the decaying pathways which are induced by the presence of the coherent driving and it is not observed (i.e., emission enhancement due to quantum interferences) for a single-atom system or an independent atomic ensemble. Finally, the scheme works as well when $\gamma_1 > \gamma_2$ or if $\omega_{31} \gg \omega_{32}$.

ACKNOWLEDGMENTS

We have benefited from useful discussions with Christoph H. Keitel, Karen Z. Hatsagortsyan, Kilian Heeg, and Jonas Gunst. Also, we are grateful for the hospitality of the Theory Division of the Max Planck Institute for Nuclear Physics in Heidelberg, Germany. Furthermore, N.C. acknowledges financial support from the National Natural Science Foundation of China (Grant No. 11404142); M.A.M. acknowledges financial support from the Max Planck Institute for Nuclear Physics and the Academy of Sciences of Moldova (Grant No. 15.817.02.09F).

[1] R. H. Dicke, Coherence in spontaneous radiation processes, Phys. Rev. **93**, 99 (1954).

[2] G. S. Agarwal, *Quantum Statistical Theories of Spontaneous Emission and their Relation to other Approaches* (Springer, Berlin, 1974).

[3] M. Gross and S. Haroche, Superradiance: An essay on the theory of collective spontaneous emission, Phys. Rep. **93**, 301 (1982).

[4] A. V. Andreev, V. I. Emel'yanov, and Y. A. Il'inskii, *Cooperative Effects in Optics: Superfluorescence and Phase Transitions* (IOP, London, 1993).

[5] Z. Ficek and S. Swain, *Quantum Interference and Coherence: Theory and Experiments* (Springer, Berlin, 2005).

[6] M. Kiffner, M. Macovei, J. Evers, and C. H. Keitel, Vacuum-induced processes in multilevel atoms, Prog. Opt. **55**, 85 (2010).

[7] J. Peng and G.-X. Li, *Introduction to Modern Quantum Optics* (World Scientific, Singapore, 1998).

[8] E. Akkermans, A. Gero, and R. Kaiser, Photon Localization and Dicke Superradiance in Atomic Gases, Phys. Rev. Lett. **101**, 103602 (2008).

[9] B. M. Garraway, The Dicke model in quantum optics: Dicke model revisited, Philos. Trans. R. Soc. A **369**, 1137 (2011).

[10] M. Nagasono, J. R. Harries, H. Iwayama, T. Togashi, K. Tono, M. Yabashi, Y. Senba, H. Ohashi, T. Ishikawa, and E. Shigemasa, Observation of Free-Electron-Laser-Induced Collective Spontaneous Emission (Superfluorescence), Phys. Rev. Lett. **107**, 193603 (2011).

[11] C. Müller, M. A. Macovei, and A. B. Voitkiv, Collectively enhanced resonant photoionization in a multiatom ensemble, Phys. Rev. A **84**, 055401 (2011).

[12] N. Brinke, R. Schützhold, and D. Habs, Feasibility study of a nuclear exciton laser, Phys. Rev. A **87**, 053814 (2013).

[13] X. Zhang and A. A. Svidzinsky, Superradiant control of γ-ray propagation by vibrating nuclear arrays, Phys. Rev. A **88**, 033854 (2013).

[14] E. Wolfe and S. F. Yelin, Certifying Separability in Symmetric Mixed States of N Qubits, and Superradiance, Phys. Rev. Lett. **112**, 140402 (2014).

[15] D. D. Yavuz, Superradiance as a source of collective decoherence in quantum computers, J. Opt. Soc. Am. B **31**, 2665 (2014).

[16] P. Longo, C. H. Keitel, and J. Evers, Tailoring superradiance to design artificial quantum systems, Sci. Rep. **6**, 23628 (2016).

[17] K. Cong, Q. Zhang, Y. Wang, G. T. Noe, A. Belyanin, and J. Kono, Dicke superradiance in solids, J. Opt. Soc. Am. B **33**, C80 (2016).

[18] C. H. Keitel, M. O. Scully, and G. Süssmann, Triggered superradiance, Phys. Rev. A **45**, 3242 (1992).

[19] V. Kozlov, O. Kocharovskaya, Y. Rostovtsev, and M. Scully, Superfluorescence without inversion in coherently driven three-level systems, Phys. Rev. A **60**, 1598 (1999).

[20] L. Yuan, D. Wang, A. A. Svidzinsky, H. Xia, O. Kocharovskaya, A. Sokolov, G. R. Welch, S. Suckewer, and M. O. Scully, Transient lasing without inversion via forbidden and virtual transitions, Phys. Rev. A **89**, 013814 (2014).

[21] J. Gunst, Y. A. Litvinov, C. H. Keitel, and A. Palffy, Dominant Secondary Nuclear Photoexcitation with the X-Ray Free-Electron Laser, Phys. Rev. Lett. **112**, 082501 (2014).

[22] K. P. Heeg, H.-C. Wille, K. Schlage, T. Guryeva, D. Schumacher, I. Uschmann, K. S. Schulze, B. Marx, T. Kämpfer, G. G. Paulus, R. Röhlsberger, and J. Evers, Vacuum-Assisted Generation and Control of Atomic Coherences at X-Ray Energies, Phys. Rev. Lett. **111**, 073601 (2013).

[23] E. Paspalakis and P. L. Knight, Phase Control of Spontaneous Emission, Phys. Rev. Lett. **81**, 293 (1998).

[24] M.-A. Bouchiat and L. Pottier, Optical experiments and weak interactions, Science **234**, 1203 (1986).

[25] M. Gunawardena and D. S. Elliott, Atomic Homodyne Detection of Weak Atomic Transitions, Phys. Rev. Lett. **98**, 043001 (2007).

[26] K. Tsigutkin, D. Dounas-Frazer, A. Family, J. E. Stalnaker, V. V. Yashchuk, and D. Budker, Observation of a Large Atomic Parity Violation Effect in Ytterbium, Phys. Rev. Lett. **103**, 071601 (2009).

[27] Y. Zhang, U. Khadka, B. Anderson, and M. Xiao, Temporal and Spatial Interference between Four-Wave Mixing and Six-Wave Mixing Channels, Phys. Rev. Lett. **102**, 013601 (2009).

[28] R. Santra, E. Arimondo, T. Ido, C. H. Greene, and J. Ye, High-Accuracy Optical Clock via Three-Level Coherence in Neutral Bosonic ^{88}Sr, Phys. Rev. Lett. **94**, 173002 (2005).

[29] M. A. Norcia, M. N. Winchester, J. R. K. Cline, and J. K. Thompson, Superradiance on the millihertz linewidth strontium clock transition, Sci. Adv. **2**, e1601231 (2016).

[30] D. Meiser, J. Ye, D. R. Carlson, and M. J. Holland, Prospects for a Millihertz-Linewidth Laser, Phys. Rev. Lett. **102**, 163601 (2009).

[31] Z. Chen and H. Freedhoff, Cooperative atomic effects in two-photon spontaneous emission and resonance fluorescence, Phys. Rev. A **44**, 546 (1991).

[32] N. Enaki and M. Macovei, Cooperative emission in the process of cascade and dipole-forbidden transitions, Phys. Rev. A **56**, 3274 (1997).

[33] A. Bakasov, N. Bogolyubov, A. Shumovskii, and V. Yukalov, Kinetics of two-photon superradiance in the case of damped polarization, Teor. Mat. Fiz. **72**, 987 (1987).

[34] G. S. Agarwal and S. Das, Electromagnetic field induced modification of branching ratios for emission in structured vacuum, New J. Phys. **10**, 013014 (2008).

[35] J. G. Bohnet, Z. Chen, J. M. Weiner, K. C. Cox, D. Meiser, M. J. Holland, and J. K. Thompson, A quasi-continuous superradiant Raman laser with < 1 intracavity photon, EPJ Web Conf. **57**, 03003 (2013).

[36] E. V. Baklanov and V. P. Chebotaev, Concerning possibility of lasing in the gamma band, JETP Lett. **21**, 131 (1975).

[37] K. Heeg, C. H. Keitel, and J. Evers, Inducing and detecting collective population inversions of Mössbauer nuclei, arXiv:1607.04116.